

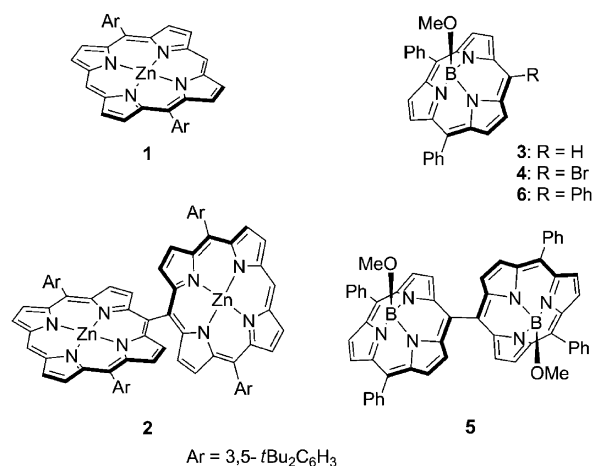
## meso-meso-Linked Subporphyrin Dimer

Masaaki Kitano,<sup>[a]</sup> Jooyoung Sung,<sup>[b]</sup> Kyu Hyung Park,<sup>[b]</sup> Hideki Yorimitsu,<sup>[a]</sup>  
Dongho Kim,<sup>\*[b]</sup> and Atsuhiko Osuka<sup>\*[a]</sup>

The subporphyrin, a genuine ring-contracted porphyrin consisting of three pyrrole units and three methine carbons, has emerged as a new functional pigment in view of its distinct  $14\pi$ -electronic aromatic system, and tunable absorption and emission properties.<sup>[1,2]</sup> In particular, *meso*-aryl substituents provide significant influences on the electronic nature of subporphyrins by virtue of their almost free rotation at room temperature, as was reported for *meso*-(oligo-1,4-phenyleneethynylene)- and *meso*-(4-aminophenyl)-substituted subporphyrins.<sup>[3]</sup> Herein, we report the synthesis of a *meso-meso* linked subporphyrin dimer **5**, which is an important molecule for comparison with the numerous examples of *meso-meso* linked  $Zn^{II}$ -porphyrin arrays already described in the literature.<sup>[4,5]</sup> Directly *meso-meso* linked  $Zn^{II}$ -diporphyrin **2** was prepared by  $Ag^I$ -promoted oxidative dimerization of  $Zn^{II}$  porphyrin **1**. In diporphyrin **2**, the two porphyrins are rigidly held at nearly perpendicular orientation with hindered rotation at the *meso-meso* linkage, which leads to minimum electronic interaction between the two porphyrins despite the direct connection.<sup>[6]</sup> The absorption spectrum of **2** shows a split Soret band, which can be interpreted in terms of simple exciton coupling of the two  $Zn^{II}$ -porphyrins without significant conjugative interaction. In line with this feature, state-to-state excitation energy hopping is common for *meso-meso* linked  $Zn^{II}$ -porphyrin arrays.<sup>[6,7]</sup>

Recently, *meso*-free and *meso*-bromosubporphyrin **3** and **4** have been explored and used for the synthesis of various *meso*- $A_2B$ -type-substituted subporphyrins.<sup>[8]</sup> By following the synthesis of **2**, we initially attempted oxidative coupling of **3**. Various oxidizing agents, such as  $AgPF_6$ ,<sup>[4]</sup>  $AgPF_6$ , and  $I_2$ ,<sup>[9a,b]</sup> and [bis(trifluoroacetoxy)iodo]benzene<sup>[9c]</sup> were trialed in attempted oxidative dimerization reactions of **3**, but the formation of **5** was not observed, and only decomposition of

**3** took place. These negative results led us to explore reductive coupling<sup>[10]</sup> of **4**. A solution of an equivalent amount of  $[Ni(cod)_2]$  and **4** in DMF was heated at  $80^\circ C$  for 2 h under argon atmosphere.<sup>[11]</sup> After usual work-up, *meso-meso* linked subporphyrin dimer **5** was obtained in 31% yield along with the recovery of **3** (27%). An excess amount of 1,5-cyclooctadiene was added with the intention of securing catalyst duration, which led to a remarkable improvement in yield of **5** (72%) with suppression of debromination (Scheme 1).



Scheme 1. Porphyrins **1**, **2** and subporphyrins **3–6**.

The high-resolution electrospray ionization time-of-flight (HR ESI-TOF) mass spectrum of **5** revealed an intense borenium cation peak at  $m/z$  817.3095 (calcd for  $C_{55}H_{35}B_2N_6O_1$  817.3070 [**5**-OMe]<sup>+</sup>). The  $^1H$  NMR spectrum of **5** shows a broad spectrum at room temperature, which has been ascribed to slow rotation of the *meso-meso* linkage comparable to NMR time scale (Figure 1). Consistent with this interpretation, **5** shows a clear  $^1H$  NMR spectrum at  $-40^\circ C$  that consists of five sets of signals due to the  $\beta$ -pyrrolic protons and two sets of signals due to the *ortho*, *meta*, and *para* protons of the *meso*-phenyl groups, differentiating the concave and convex sides of the bowl-shaped subporphyrin macrocycle (Figure 1). Characteristically, a signal due to  $H^6$  at the concave face is upfield shifted, and  $H^1$  and  $H^2$  at the convex face are downfield shifted. At  $120^\circ C$ , the  $^1H$  NMR spectrum of **5** became simpler due to smooth rotation of the *meso-meso* linkage. These rotational features of **5** are distinctly different from those of **2**.

[a] M. Kitano, Prof. Dr. H. Yorimitsu, Prof. Dr. A. Osuka  
Department of Chemistry, Graduate School of Science  
Kyoto University, Sakyo-ku, Kyoto 606-8502 (Japan)  
Fax: (+81) 75-753-3970  
E-mail: osuka@kuchem.kyoto-u.ac.jp

[b] J. Sung, K. H. Park, Prof. Dr. D. Kim  
Department of Chemistry and Spectroscopy of  
 $\pi$ -Functional Electronic System, Yonsei University  
Seoul 120-749, (Korea)  
E-mail: dongho@yonsei-u.ac.kr

Supporting information for this article is available on the WWW under <http://dx.doi.org/10.1002/chem.201303767>.

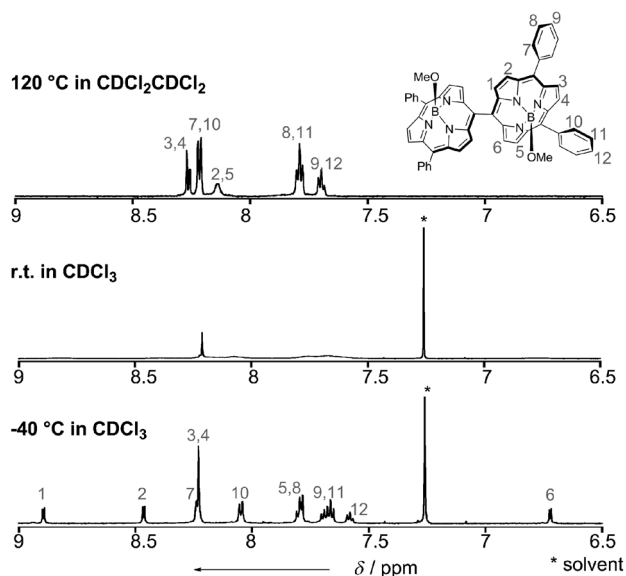


Figure 1.  $^1\text{H}$  NMR spectra of **5** at various temperatures.

To evaluate the rotation barrier of the *meso-meso* linkage, *meso-meso* linked subporphyrin dimer **7** was prepared by the same method, which displays a singlet signal due to the tolyl protons. Similar to **5**, the  $^1\text{H}$  NMR spectrum of **7** exhibits temperature-dependent spectral changes. By simulating the observed spectral changes of signals due to the tolyl proton of **7** (Figure 2),<sup>[12]</sup> the values for  $\Delta H^\ddagger$ ,  $\Delta S^\ddagger$ , and  $\Delta G_{298}^\ddagger$  of the rotation barrier have been determined to be  $14.7 \text{ kcal mol}^{-1}$ ,  $1.28 \text{ cal mol}^{-1} \text{ K}^{-1}$ , and  $14.3 \text{ kcal mol}^{-1}$ , respectively.

Subporphyrin dimer **5** was converted to its B,B'-dibenzyl-oxy congener **5-OBn** by heating in the presence of benzyl alcohol. Slow recrystallization from a mixture of  $\text{CHCl}_3$  and toluene gave nice crystals of **5-OBn**. Single-crystal XRD

analysis revealed a directly *meso-meso* linked dimer structure, in which the mean bowl depth is  $1.33 \text{ \AA}$  and the center-to-center distance (B–B distance) is  $7.21 \text{ \AA}$  and the C(*meso*)–C(*meso*) bond length is  $1.48 \text{ \AA}$ , and the dihedral angle between the two subporphyrin cores is  $55.5^\circ$  (Figure 3).<sup>[13]</sup> The C(*meso*)–C(*meso*) bond length of **5-OBn** is similar to that ( $1.47 \text{ \AA}$ ) of *meso-meso* linked  $\text{Zn}^{\text{II}}$ -diporphyrin **2**, but the dihedral angle of **5-OBn** is considerably smaller than that ( $86.1^\circ$ ) of **2**. The latter structural feature may lead to stronger electronic interaction between the two subporphyrin units.

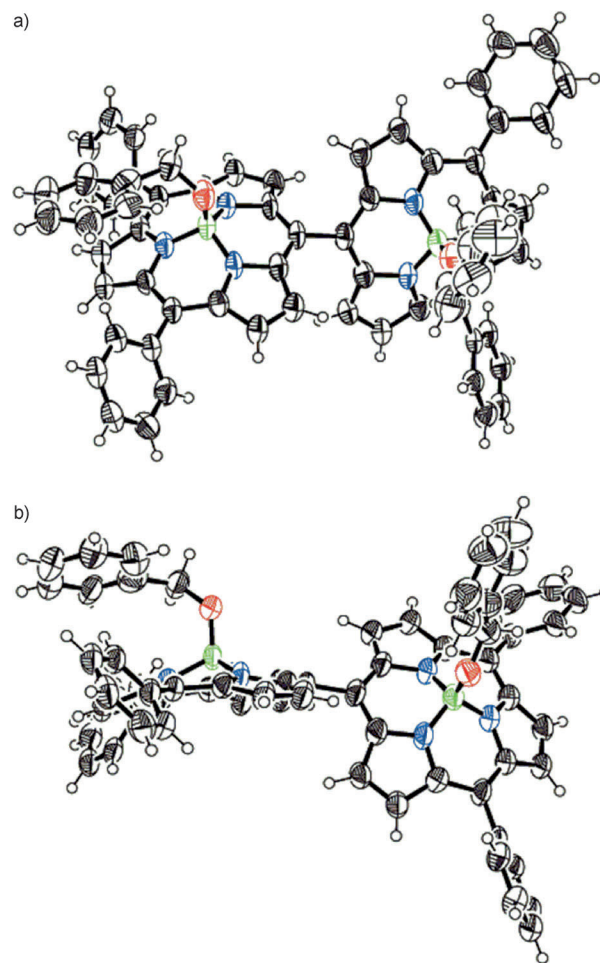


Figure 3. X-ray crystal structure of **5-OBn**: a) perspective and b) side views. Thermal ellipsoids are represent 50% probability. Solvent molecules are omitted for clarity.

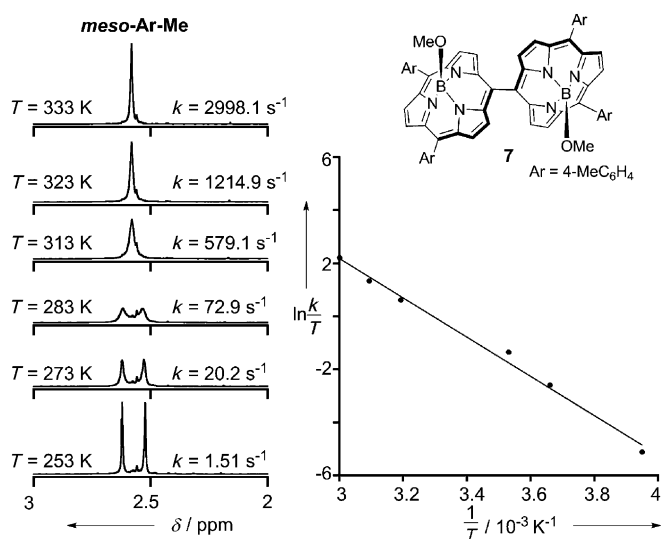


Figure 2. Temperature-dependent  $^1\text{H}$  NMR spectral changes of the methyl group of **7** (left) and a plot of  $\ln(k/T)$  versus  $1/T$  (right).

The UV/Vis absorption spectra of **5** and its reference monomer **6** in toluene are shown in Figure 4. Although the subporphyrin monomer **6** shows a Soret-like band at  $375 \text{ nm}$  and Q-like bands at  $462$  and  $486 \text{ nm}$ , that of *meso-meso* linked dimer **5** is significantly altered, featuring a Soret-like band at  $403 \text{ nm}$  with a broad shoulder around  $388 \text{ nm}$  and broadened Q-like bands with peaks at  $462$  and  $516 \text{ nm}$  and a tail extending over  $550 \text{ nm}$ . These absorption features suggest stronger electronic interactions in **5** than those in **2**.

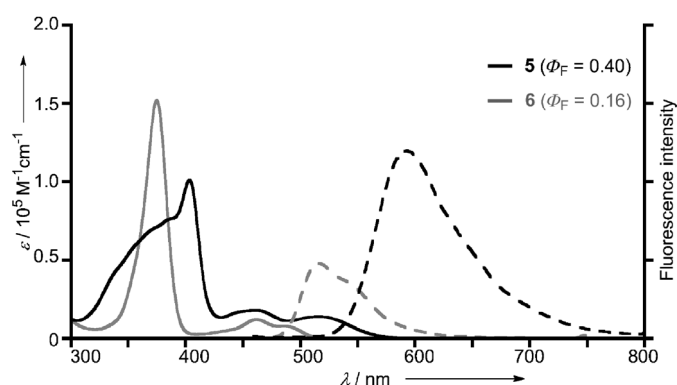


Figure 4. UV/Vis absorption (solid lines) and fluorescence (dashed lines) spectra of **5** and its reference monomer **6** in toluene.

The absorption spectrum of **2** displays a split Soret band at 416 and 451 nm and slightly redshifted Q bands, which has been interpreted in terms of exciton coupling with negligible conjugative interaction.<sup>[5,6]</sup> Therefore, conjugative interactions of the two subporphyrin units are suggested for **5** in addition to excitonic interaction. Fluorescence spectrum of **5** in toluene is largely redshifted to 593 nm and is substantially enhanced ( $\Phi_F=0.40$ ) with a large Stokes shift ( $2520\text{ cm}^{-1}$ ), compared to that of **6** (at 517 nm,  $\Phi_F=0.16$ , and  $1230\text{ cm}^{-1}$ ). Such large changes in the fluorescence spectrum were not observed for **2**. Fluorescence lifetime of **5** has been determined by single-photon counting to be 2.3 ns, which is slightly shorter than that (2.8 ns) of **6**. The fluorescence spectrum of **5** is rather insensitive to solvent polarity and did not show quenching even in polar solvents such as THF and DMSO, different from recently reported boron-dipyrromethene (BODIPY) dimers.<sup>[14]</sup> This has been ascribed to small  $S_1$ -excitation energy of **5** (2.09 eV) due to large electronic interaction, which is not sufficient to induce so-called symmetry-breaking intramolecular charge separation.<sup>[15]</sup>

The transient absorption spectra in toluene after photoexcitation at 540 nm were recorded (Figure 5). Characteristically, the transient stimulated emission (SE) band of **5** was clearly observed, and its peak position was gradually redshifted in 30 ps time range, whereas SE band of **6** was very weak, and the excited state absorption spectra did not show a significant spectral shift. We can suggest that this dynamic Stokes shift of  $S_1$  fluorescence in **5** is probably caused by continuous structural changes of dihedral angle in the excited state. These features are distinct characteristics of **5**, not observed for **2**. Because of rigid and orthogonal geometry of **2**, the molecular orbital (MO) interaction between the two porphyrin cores is weak.<sup>[16]</sup> However, the situation is different for **5**, in which the rotation around the direct meso-meso linkage leads to efficient MO interactions between the constituent subporphyrins. It is conceivable that the torsional relaxation after photoexcitation may cause more coplanar geometry, and the  $Q_z$  ( $z$  direction along the long molecular axis) state transition becomes stabilized and enhanced by increasing electronic communication between the two subporphyrins cores.<sup>[17]</sup> Therefore, the enhanced  $Q_z$  state transition

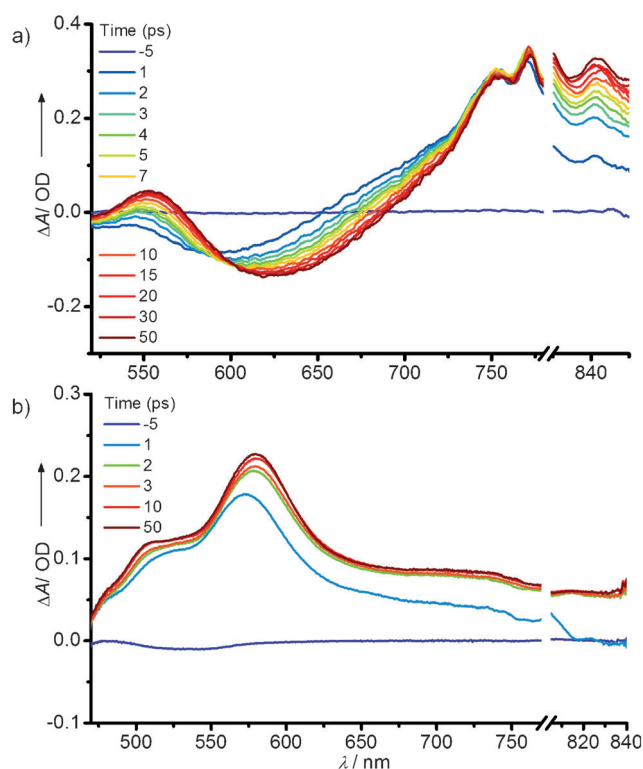


Figure 5. Transient absorption spectra of a) **5** and b) **6** in toluene obtained by photoexcitation at  $\lambda=510$  and 460 nm, respectively.

and large oscillator strength of **5** can explain the observed large  $S_1$  fluorescence quantum yield and clear dynamic Stokes shift of SE bands.

Interestingly, the anisotropy decay profile of **5** is distinctly different from those of **2** and **6** (Figure 6).<sup>[6]</sup> The anisotropy decay profile of **6** shows an initial anisotropy value of 0.1 resulting from an ultrafast in-plane dephasing process between  $Q_x$  and  $Q_y$  transitions. The anisotropy decay profile of diporphyrin **2** revealed an ultrafast depolarization process, in which anisotropy value decreases from 0.4 to 0.04 with

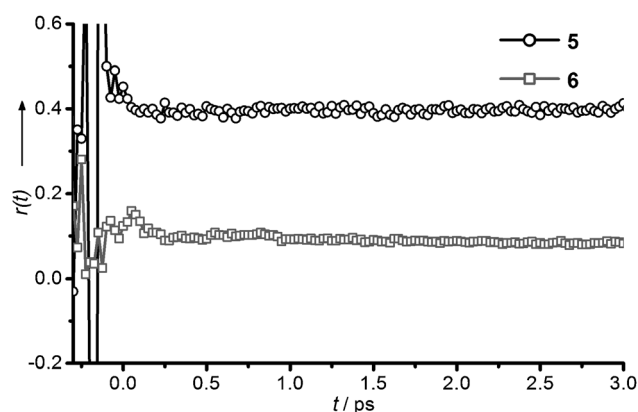


Figure 6. Temporal profiles of femtosecond transient absorption anisotropy decays of **5** (black) and **6** (gray) in toluene monitoring at  $\lambda=620$  and 580 nm with photoexcitation of Q bands at  $\lambda=540$  and 480 nm, respectively.

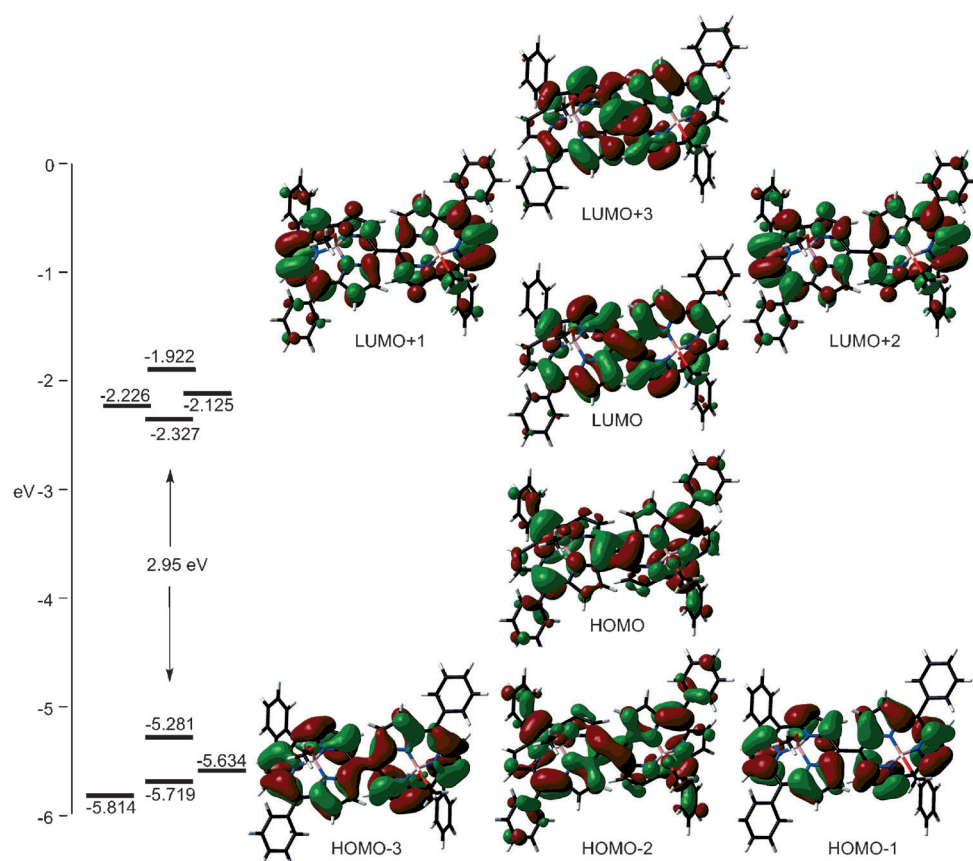


Figure 7. MO diagrams of **5** calculated with Gaussian 09 package (all energy levels were calculated at the B3LYP/6-311G(d) level. Each MO was visualized with cubegen program).<sup>[20]</sup>

a time constant of < 200 fs.<sup>[18]</sup> Such a fast depolarization process is attributable to a mixing of all relaxation processes, such as in-plane dephasing of  $Q_x$  and  $Q_y$  in porphyrin monomer, energy hopping between the two transition dipoles, and internal conversion from  $Q_x$  or  $Q_y$  state of monomeric unit to  $Q_z$  state of the dimer.<sup>[6]</sup> Likewise, porphyrin arrays holding monomeric character are known to show complicated depolarization processes due to ultrafast dephasing of the two degenerate transition dipoles in the porphyrin monomer, as well as the energy transfer between the porphyrin monomers.<sup>[18,19]</sup> In contrast, the anisotropy decay profile of subporphyrin dimer **5** shows a high initial anisotropy value of 0.4 and slow single exponential decay with a time constant of 300 ps. This slow decay can be assigned as a rotational diffusion. Based on this high initial anisotropy value and rather simple depolarization process of **5**, we can propose that the  $\pi$  conjugation extends to the whole molecule, and hence **5** can be regarded as a one-quantum system.

The molecular structures and MO diagrams of **5** were optimized at B3LYP/6-311G(d) level by using the Gaussian 09 package (Figure 7).<sup>[20]</sup> We have previously reported that *meso*-triphenyl-substituted subporphyrin **6** possesses quite porphyrin-like four orbitals,  $a_{1u}$ -like HOMO-1,  $a_{2u}$ -like HOMO, and  $e_g$ -like LUMO and LUMO+1.<sup>[2b,21]</sup> The HOMO and LUMO of subporphyrin dimer **5** are both

spread over the two subporphyrin units, indicating the delocalized nature of electronic states of **5**.

The electrochemical properties of **5** were examined by cyclic voltammetry (CV) in  $\text{CH}_2\text{Cl}_2$  containing 0.1 M  $\text{Bu}_4\text{NPF}_6$  as a supporting electrolyte versus ferrocene/ferrocenium cation (see the Supporting Information). One-electron oxidation waves of **5** were observed at 0.60 and 1.03 V, and reduction wave was observed at -1.78 V, whereas those of **6** were observed at 0.82 and -1.84 V. These data allowed us to determine the electrochemical HOMO-LUMO gaps of **5** and **6** to be 2.38 and 2.66 eV, respectively. The two oxidation waves of **5** have been assigned as split first oxidation waves (one electron per subporphyrin), as was judged from the results of other electronically interacting diporphyrins.<sup>[22]</sup> Potential difference between the first and second oxidation waves ( $\Delta E = E_{\text{OX2}} - E_{\text{OX1}}$ ) of **5** is 0.43 V, which is substantially larger than that (0.11 V) of **2** and is comparable with that (0.42 V) of a fully conjugated  $\text{Zn}^{\text{II}}$  porphyrin tape, again supporting the large electronic interaction in **5**.<sup>[22]</sup>

In summary, directly *meso-meso* linked subporphyrin dimer **5** and **7** were synthesized by Ni-mediated reductive coupling of the corresponding *meso*-bromosubporphyrins. Dimer **5** exhibited a largely perturbed absorption spectrum, a redshifted and enhanced fluorescence spectrum, higher oxidation potentials with a large potential difference between

the first and second oxidation waves, and a long-lived large anisotropy of  $S_1$  state. These properties have been interpreted in terms of the effective conjugative interactions of the two subporphyrin units due to the small rotational barrier of the meso-meso bond. Exploration of more elaborated systems, such as meso-meso linked subporphyrin oligomers and porphyrin-subporphyrin hybrids, are actively pursued in our laboratories.

### Acknowledgements

The work at Kyoto was supported by Grant-in-Aid (No. 25220802(S)) for Scientific Research from MEXT of Japan. M.K. acknowledges a JSPS Fellowship for Young Scientists. The work at Yonsei was supported by the Global Frontier R&D Program of the Center for Multiscale Energy System (2012-8-2081), Mid-career Researcher Program (2010-0029668) of National Research Foundation (NRF) grant funded by MEST of Korea, and AFSOR/AOARD grant (no. FA2386-09-4092).

**Keywords:** anisotropy • conjugative interaction • porphyrinoids • reductive coupling • subporphyrins

- [1] a) Y. Inokuma, A. Osuka, *Dalton Trans.* **2008**, 2517; b) T. Torres, *Angew. Chem.* **2006**, *118*, 2900; *Angew. Chem. Int. Ed.* **2006**, *45*, 2834; c) A. Osuka, E. Tsurumaki, T. Tanaka, *Bull. Chem. Soc. Jpn.* **2011**, *84*, 679.
- [2] a) Y. Inokuma, J. H. Kwon, T. K. Ahn, M.-C. Yoo, D. Kim, A. Osuka, *Angew. Chem.* **2006**, *118*, 975; *Angew. Chem. Int. Ed.* **2006**, *45*, 961; b) Y. Inokuma, Z. S. Yoon, D. Kim, A. Osuka, *J. Am. Chem. Soc.* **2007**, *129*, 4747; c) N. Kobayashi, Y. Takeuchi, A. Matsuda, *Angew. Chem.* **2007**, *119*, 772; *Angew. Chem. Int. Ed.* **2007**, *46*, 758; d) Y. Takeuchi, A. Matsuda, N. Kobayashi, *J. Am. Chem. Soc.* **2007**, *129*, 8271.
- [3] a) Y. Inokuma, S. Easwaramoorthi, S. Y. Jang, K. S. Kim, D. Kim, A. Osuka, *Angew. Chem.* **2008**, *120*, 4918; *Angew. Chem. Int. Ed.* **2008**, *47*, 4840; b) Y. Inokuma, S. Easwaramoorthi, Z. S. Yoon, D. Kim, A. Osuka, *J. Am. Chem. Soc.* **2008**, *130*, 12234.
- [4] a) A. Osuka, H. Shimidzu, *Angew. Chem.* **1997**, *109*, 93; *Angew. Chem. Int. Ed. Engl.* **1997**, *36*, 135; b) A. Nakano, A. Osuka, I. Yamazaki, T. Yamazaki, Y. Nishimura, *Angew. Chem.* **1998**, *110*, 3172; *Angew. Chem. Int. Ed.* **1998**, *37*, 3023; c) N. Aratani, A. Osuka, Y. H. Kim, D. H. Jeong, D. Kim, *Angew. Chem.* **2000**, *112*, 1517; *Angew. Chem. Int. Ed.* **2000**, *39*, 1458.
- [5] a) N. Aratani, A. Osuka, *Bull. Chem. Soc. Jpn.* **2001**, *74*, 1361; b) D. Kim, A. Osuka, *Acc. Chem. Res.* **2004**, *37*, 735; c) N. Aratani, D. Kim, A. Osuka, *Acc. Chem. Res.* **2009**, *42*, 1922.
- [6] a) Y. H. Kim, D. H. Jeong, D. Kim, S. C. Jeoung, H. S. Cho, S. K. Kim, N. Aratani, A. Osuka, *J. Am. Chem. Soc.* **2001**, *123*, 76; b) D. Kim, A. Osuka, *J. Phys. Chem. A* **2003**, *107*, 8791.
- [7] N. Aratani, H. S. Cho, T. K. Ahn, S. Cho, D. Kim, H. Sumi, A. Osuka, *J. Am. Chem. Soc.* **2003**, *125*, 9668.
- [8] a) M. Kitano, S. Hayashi, T. Tanaka, H. Yorimitsu, N. Aratani, A. Osuka, *Angew. Chem.* **2012**, *124*, 5691; *Angew. Chem. Int. Ed.* **2012**, *51*, 5593; b) T. Tanaka, M. Kitano, S. Hayashi, N. Aratani, A. Osuka, *Org. Lett.* **2012**, *14*, 2694; c) M. Kitano, S. Hayashi, T. Tanaka, N. Aratani, A. Osuka, *Chem. Eur. J.* **2012**, *18*, 8929.
- [9] a) A. Nakano, H. Shimidzu, A. Osuka, *Tetrahedron Lett.* **1998**, *39*, 9489; b) X. Shi, L. S. Liebeskind, *J. Org. Chem.* **2000**, *65*, 1665; c) L.-M. Jin, L. Chen, J.-J. Yin, C.-C. Guo, Q.-Y. Chen, *Eur. J. Org. Chem.* **2005**, 3994.
- [10] X.-Q. Lu, Y. Guo, Q.-Y. Chen, *Synlett* **2011**, 77.
- [11] M. F. Semmelhack, P. M. Helquist, L. D. Jones, *J. Am. Chem. Soc.* **1971**, *93*, 5908.
- [12] F. P. Gasparro, N. H. Kolodny, *J. Chem. Educ.* **1977**, *54*, 258.
- [13] Crystal data for **5-OBn**:  $C_{68}H_{46}B_2N_6O_2 \cdot 2C_7H_8$ ;  $M_w = 1185.00$ ; triclinic; space group  $P\bar{1}$  (No. 2);  $a = 12.1018(3)$ ,  $b = 15.8455(3)$ ,  $c = 17.9185(4)$  Å;  $\alpha = 103.4753(13)$ ,  $\beta = 104.6738(13)$ ,  $\gamma = 103.5719(13)^\circ$ ;  $V = 3070.89(12)$  Å<sup>3</sup>;  $T = 93$  K;  $\rho_{\text{calcd}} = 1.282$  g cm<sup>-3</sup>;  $Z = 2$ ; 28270 reflections measured; 9528 unique ( $R_{\text{int}} = 0.0786$ );  $R_1 = 0.0992$  [ $I > 2.0\sigma(I)$ ];  $wR_2 = 0.3195$  (all data); GOF = 1.075. CCDC-931802 contains the supplementary crystallographic data for this paper. These data can be obtained free of charge from The Cambridge Crystallographic Data Centre via [www.ccdc.cam.ac.uk/data\\_request/cif](http://www.ccdc.cam.ac.uk/data_request/cif).
- [14] M. T. Whited, N. M. Patel, S. T. Roberts, K. Allen, P. J. Djurovich, S. E. Bradforth, M. E. Thompson, *Chem. Commun.* **2012**, 48, 284.
- [15] a) W. Rettig, *Angew. Chem.* **1986**, *98*, 969; *Angew. Chem. Int. Ed. Engl.* **1986**, *25*, 971; b) F. Schneider, E. Lippert, *Ber. Bunsen-Ges.* **1968**, *72*, 1155; c) N. Nakashima, M. Murakawa, N. Mataga, *Bull. Chem. Soc. Jpn.* **1976**, *49*, 854.
- [16] T. Miyahara, H. Nakatsuji, J. Hasegawa, A. Osuka, N. Aratani, A. Tsuda, *J. Chem. Phys.* **2002**, *117*, 11196.
- [17] a) S. Cho, M.-C. Yoon, K. S. Kim, P. Kim, D. Kim, *Phys. Chem. Chem. Phys.* **2011**, *13*, 16175; b) G. Duvanel, J. Crilj, A. Schuwey, A. Gossauer, E. Vauthey, *Photochem. Photobiol. Sci.* **2007**, *6*, 956.
- [18] a) K. Wynne, R. M. Hochstrasser, *Chem. Phys.* **1993**, *171*, 179; b) R. Kumble, S. Palese, V. S.-Y. Lin, M. J. Therien, R. M. Hochstrasser, *J. Am. Chem. Soc.* **1998**, *120*, 11489; c) H. S. Cho, N. W. Song, Y. H. Kim, S. C. Jeoung, S. Hahn, D. Kim, S. K. Kim, N. Yoshida, A. Osuka, *J. Phys. Chem. A* **2000**, *104*, 3287.
- [19] a) M.-C. Yoon, S. Cho, P. Kim, T. Hori, N. Aratani, A. Osuka, D. Kim, *J. Phys. Chem. B* **2009**, *113*, 15074; b) I.-W. Hwang, D. M. Ko, T. K. Ahn, Z. S. Yoon, D. Kim, X. Peng, N. Aratani, A. Osuka, *J. Phys. Chem. B* **2005**, *109*, 8643.
- [20] Gaussian 09, Revision A.02, M. J. Frisch, G. W. Trucks, H. B. Schlegel, G. E. Scuseria, M. A. Robb, J. R. Cheeseman, G. Scalmani, V. Barone, B. Mennucci, G. A. Petersson, H. Nakatsuji, M. Caricato, X. Li, H. P. Hratchian, A. F. Izmaylov, J. Bloino, G. Zheng, J. L. Sonnenberg, M. Hada, M. Ehara, K. Toyota, R. Fukuda, J. Hasegawa, M. Ishida, T. Nakajima, Y. Honda, O. Kitao, H. Nakai, T. Vreven, J. A. Montgomery, Jr., J. E. Peralta, F. Ogliaro, M. Bearpark, J. J. Heyd, E. Brothers, K. N. Kudin, V. N. Staroverov, R. Kobayashi, J. Normand, K. Raghavachari, A. Rendell, J. C. Burant, S. S. Iyengar, J. Tomasi, M. Cossi, N. Rega, J. M. Millam, M. Klene, J. E. Knox, J. B. Cross, V. Bakken, C. Adamo, J. Jaramillo, R. Gomperts, R. E. Stratmann, O. Yazyev, A. J. Austin, R. Cammi, C. Pomelli, J. W. Ochterski, R. L. Martin, K. Morokuma, V. G. Zakrzewski, G. A. Voth, P. Salvador, J. J. Dannenberg, S. Dapprich, A. D. Daniels, Ö. Farkas, J. B. Foresman, J. V. Ortiz, J. Cioslowski, D. J. Fox, Gaussian, Inc., Wallingford CT, **2009**.
- [21] M. Gouterman, *J. Mol. Spectrosc.* **1961**, *6*, 138.
- [22] A. Tsuda, H. Furuta, A. Osuka, *J. Am. Chem. Soc.* **2001**, *123*, 10304.

Received: September 26, 2013  
Published online: November 4, 2013